

# Physical Layer Design of Energy-Efficient Data Transmission in 2D Communication Environments

Yuichi Masuda, Hiroyuki Shinoda  
 Graduate School of Frontier Sciences  
 The University of Tokyo  
 Tokyo, Japan  
 masuda@hapis.k.u-tokyo.ac.jp,  
 hiroyuki\_shinoda@k.u-tokyo.ac.jp

**Abstract**—This paper proposes a method to determine a physical layer (PHY) parameter that minimizes energy-per-bit rate (EBR) in a two-dimensional communication (2DC) environment. EBR is the power consumption used for 1-bit transmission/reception. 2DC uses a sheet-like waveguide medium, which guides the microwave along the sheet. In our previous work, the possibility of energy-efficient data transmission by using TransferJet devices in 2DC environment was reported. The reported maximum transmission rate was 71.1 Mbps with a power consumption of 118 mW. The EBR was two orders of magnitude lower than that of ZigBee despite the same power consumption. However, the data rate significantly degraded at some transceiver positions depending on the delay spread of the 2DC channel. The decrease of the transmission rate was caused by a mismatch between the PHY parameter of the communication system and the characteristics of the communication environment. This paper presents a method to determine an optimum PHY parameter for minimizing EBR. The experimental results demonstrate the feasibility of the energy-efficient data transmission in 2DC environments.

**Keywords**—Two-dimensional communication, ultra-wideband radio, PHY protocol, software-defined radio, GNU Radio

## I. INTRODUCTION

Two-dimensional communication (2DC) is a short-range wireless communication scheme using a sheet-like waveguide medium [1]. The guided mode of this waveguide medium resembles a parallel-plate waveguide mode. Most of the energy fed into the waveguide sheet is confined in the sheet. The rest of the energy propagates as an evanescent field on the sheet. A device placed on the sheet can communicate through the sheet using proximity coupling.

The evanescent field is drastically attenuated with distance in the direction directly above the sheet. However, the attenuation of the guided mode propagating along the sheet is less than that of the over-the-air (OTA) communication environment. Thus, 2DC enables low-emission communication such as ultra wideband (UWB) radio [2].

In the previous works, the possibility of high-speed and low-power communication in the 2DC environments was reported in [3]. By using commercially available TranferJet [4] adapters in 2DC environments, the transmission rate obtained in the experiments was in the range of 24 Mbps to 71.1 Mbps according to the coupler positions with a power consumption of 118 mW [3]. The energy-per-bit rate (EBR), which is the ratio of the power

Akihito Noda  
 Department of Mechatronics  
 Nanzan University  
 Nagoya, Japan  
 anoda@nanzan-u.ac.jp

consumption to the transmission rate, was in the range of 1.7 nJ/bit to 5.0 nJ/bit. Even in the worst EBR of 5.0 nJ/bit, the EBR is 1–2 orders of magnitude lower than that of ZigBee [5]. These results show that high energy-efficient wireless communication is possible in the 2DC environment.

The ensuing subject of interest would be the theoretical limit of EBR for the optimal physical layer (PHY) parameters selected for a 2DC environment, considering the delay spread and signal-to-noise ratio (SNR) for a typical 2DC sheet. In this paper, we present a method to determine the optimum PHY parameters to minimize the EBR. Using the determined parameters, the numerical simulation shows that a transmission rate of 36 Mbps is achieved with a power consumption of 24 mW. EBR is 0.66 nJ/bit. This transmission rate was supported by the experiments. These results present the feasibility of energy-efficient communication in 2DC.

The rest of this paper is organized as follows. In Section II, a brief review of the previous 2DC works is presented. A PHY design that minimizes the EBR is shown in Section III. The experimental verification is presented in Section IV. Finally, Section V concludes this paper.

The contents of this paper have been published in part in Japanese [7]. This paper is the first publication in English.

## II. PREVIOUS WORK OF 2DC

### A. Two-dimensional Communication (2DC)

As mentioned above, 2DC environment enables the use of UWB in the range of 3.1 to 10.6 GHz. Moreover, the influence of inter-symbol interference (ISI) is less than ordinary room-scale ( $50\text{--}150\text{ m}^2$ ) OTA communication environment. The bit error caused by ISI is increased by increasing the ratio of root-mean-square (RMS) delay spread to symbol duration time  $S_{DT}$ . The RMS delay spread  $\sigma_\tau$  of a 50-cm square sheet is approximately 8–10 ns whereas the RMS delay spread of room-scale OTA environment is approximately 100–150 ns [6]. Therefore, high-speed communication with high symbol rate  $S_R (= 1/S_{DT})$  can be realized in 2DC environments. Moreover, it can reduce the power consumption of a digital signal processor because it does not require the high calculation cost of secondary modulation loading such as orthogonal frequency-division multiplexing.

## B. Active Tile 2DC

An overview of active tile 2DC is shown in Fig. 1. The communication range can be extended by spreading 50-cm square 2DC tiles on the floor [8]. Moreover, it is possible to extend the communication range to a desktop or shelf by laying communication sheets on them. The 2DC tile has a three-layer structure, which includes a carpet layer, 2DC sheet layer, and base layer. In the base layer, an amplifier circuit compensates the attenuation caused at the inter-tile connection.

In general, the RMS delay spread is scaled up by increasing the size of the communication environment. However, the RMS delay spread of the 2DC tile system is not scaled up by increasing the number of tiles. The RMS delay spread is maintained at approximately 10 ns [6] since each tile is electromagnetically independent. Thus, high-speed low-radiation communication can be achieved even for terminals that are either several meters away from each other or on a single tile.

## III. PHY DESIGN MINIMIZING EBR

This section presents a method for determining PHY parameters that minimize EBR. Specifically,  $E_b$  and  $S_R$ , which minimize EBR, are determined by solving the trade-off problem between transmission data rate and power consumption. Further,  $E_b$  denotes the received energy per bit.

The EBR is expressed as follows.

$$R_{EBR} = \frac{W}{T}, \quad (1)$$

where  $R_{EBR}$  denotes the value of EBR,  $W$  denotes the power consumption, and  $T$  denotes the transmission data rate.

### A. Definition of data rate and power consumption

In this study, the theoretical limit of transmission rate (channel capacity  $C$ ) is evaluated based on the entropy [9] as

$$C = H(Y) - H(Y|X), \quad (2)$$

where  $X$  and  $Y$  denote the transmitted and received codes, respectively, and  $H(Y)$  denotes the information bits received from the information source per second. Thus,  $H(Y)$  is expressed as follows.

$$H(Y) = kS_R, \quad (3)$$

where  $k$  denotes the value of bits per symbols. The lost entropy  $H(Y|X)$  in a communication path with the bit error rate (BER)  $\rho$  expressed as follows.

$$\begin{aligned} & H(Y|X) \\ &= kS_R\{(1 - \rho)(-\log_2(1 - \rho)) + \rho(-\log_2 \rho)\}. \end{aligned} \quad (4)$$

Notably,  $C$  determines the upper bound of the number of bits that can be transmitted per second, which also includes the error correction code and the number of bits used for the frame. In this study, we focus on the effect of PHY parameters. The influence of an upper layer such as the media access control (MAC) layer is not considered here.

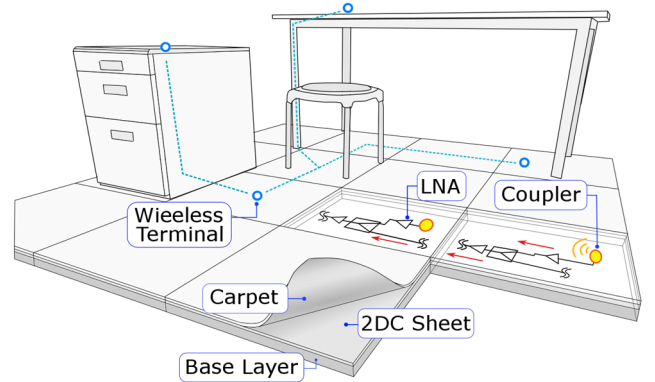


Fig. 1. Overview of active tile 2DC. In the base layer, a low noise amplifier (LNA) circuit compensates attenuation caused at the inter-tile connection. This figure is cited from [7].

Subsequently, we describe the derivation of the BER. In general, there are some factors influencing BER. If the BER caused by independent factors is sufficiently smaller than 1, BER is obtained as their sum. Further  $\rho$  and  $\rho_{SN}$ , which is the BER caused by SNR, are defined as

$$\rho = \rho_{SN} + \rho_{ISI}, \quad (5)$$

$$\text{where } \rho_{SN} = \frac{1}{2} \operatorname{erfc} \left( \sqrt{k \frac{E_b}{N_0}} \right), \quad (6)$$

where  $\rho_{ISI}$  is the BER caused by ISI and  $N_0$  donates the thermal noise power in a bandwidth of 1 Hz. Further,  $\rho_{SN}$  has different representation methods depending on the modulation system. We assume binary phase-shift keying (BPSK) modulation in this study.

An equivalent transmission path (ETP) model [10] described a propagation environment by using two waves—a leading wave and a delayed wave. A key parameter that determines  $\rho_{ISI}$  is the RMS delay spread  $\sigma_\tau$  in the Rayleigh fading environment. The ETP model can significantly simplify the description of a propagation channel, while it conserves the essential parameter  $\sigma_\tau$ .

The variable  $r$  is defined as the ratio of amplitude of the leading wave to that of the delayed wave. Further,  $\phi$  is a phase difference between the leading wave and delayed wave. The delay time of the delayed wave is denoted as  $\Delta\tau$ . The value of  $\rho_{ISI}$  when the aforementioned variables assume a certain value is expressed as  $P_0\{r, \phi; \Delta\tau(\sigma_\tau)\}$ . For  $\sigma_\tau/S_{DT} < 0.5$ , the probability density function of the aforementioned variables is expressed as

$$f_R\{r, \phi; \sigma_\tau\} = \frac{1}{\pi} \frac{r}{(r^2 + 1)^2}, \quad (7)$$

where  $\phi$  follows a uniform distribution in the Rayleigh fading. In general, assuming Rayleigh fading,  $f_R$  is independent of  $\sigma_\tau$ .

We define  $f_R'\{r; \sigma_\tau\}$  as follows.

$$f_R'\{r; \sigma_\tau\} = \int_0^{2\pi} f_R\{r, \phi; \sigma_\tau\} d\phi = \frac{2r}{(r^2 + 1)^2}. \quad (8)$$

The variable  $\Delta\tau$  is expressed as follows.

$$\Delta\tau = 2\sigma_\tau. \quad (9)$$

Further,  $\rho_{ISI}$  is obtained as the product of  $P_0$  and  $f_R$ . Based on the above discussion,  $\rho_{ISI}$  is expressed as follows.

$$\begin{aligned} \rho_{ISI}(\sigma_\tau) \\ = \int_0^\infty f_R'(r; \sigma_\tau) \left( \int_0^{2\pi} P_0\{r, \phi; \Delta\tau(\sigma_\tau)\} d\phi \right) dr. \end{aligned} \quad (10)$$

In (10),  $P_0$  is obtained by using simulation software, which calculates the BER of a communication system.  $P_0$  calculated in the  $r$ - $\phi$  plane is called the BER map [10]. BER map must be calculated according to each  $\Delta\tau$ , which differs for every  $\sigma_\tau$ . An approximate equation by using only one BER map is proposed in [11] to decrease the calculation load in creating many BER maps. It uses the shape correlation between  $\Delta\tau$  and the BER map.

Further,  $P_0\{x, \phi; \Delta\tau_{map}\}$  denotes a BER map in the approximate equation of (9),  $\Delta\tau_{map}$  denotes  $\Delta\tau$  in a BER map,  $x$  is the logarithmic expression of  $r$ , and  $x$  and  $\phi$  are discrete values with the step widths of  $\Delta x$  and  $\Delta\phi$ , respectively. If  $\Delta\tau_{map}/S_{DT} < 0.5$ , the value of  $\Delta\tau_{map}$  can be set arbitrarily. Moreover,  $\Delta\tau_{map}/S_{DT} = 0.2$  is recommended [12] and we followed it. The range of  $x$  and  $\phi$  is assumed until  $P_0$  is sufficiently close to 0. We set the range of  $x$  from -7.5 to 7.5 with  $\Delta x = 0.25$ . Furthermore, the range of  $\phi$  is set from 90° to 270° with  $\Delta\phi = 2^\circ$ . Based on the above discussion,  $\rho_{ISI}$  is expressed as follows.

$$\rho_{ISI}(\sigma_\tau) \approx \eta^2 \Delta x \Delta \phi \sum_x g_R(\eta x) \left( \sum_\phi P_0\{x, \phi; \Delta\tau_{map}\} \right), \quad (11-1)$$

$$\eta = \frac{2\sigma_\tau}{\Delta\tau_{map}}, \quad (11-2)$$

$$g_R(x) = \frac{1}{b} \exp\left(\frac{x}{b}\right) f'_R\left\{\exp\left(\frac{x}{b}\right); \sigma_\tau\right\}, \quad (11-3)$$

where  $b \equiv 20 \log_{10} e$ .

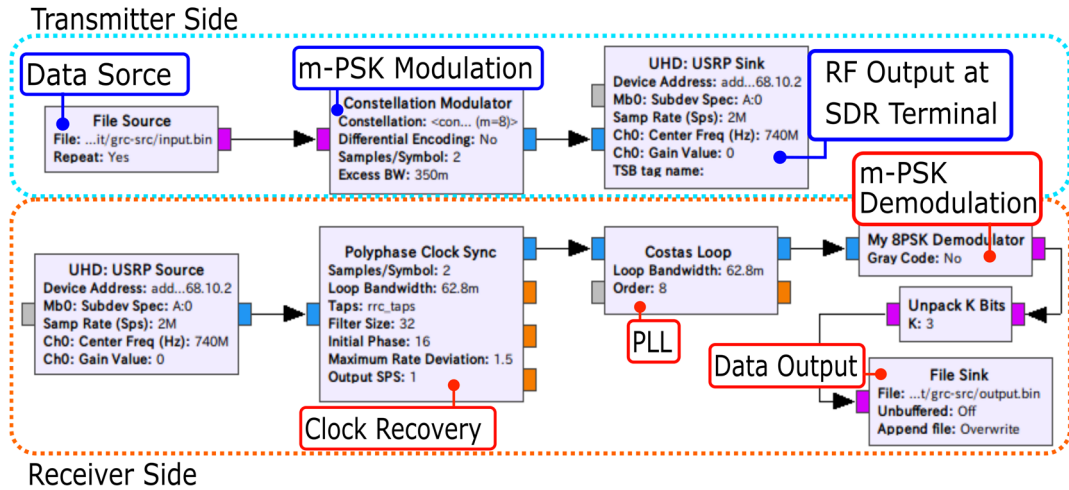


Fig. 2. Flow diagram of prototype system in GNU Radio. This figure is cited from [7].

The power consumption is the sum of the RF component  $W_{RF}$  and digital component  $W_{DSP}$  expressed as follows.

$$W = W_{RF} + W_{DSP}. \quad (12)$$

Further,  $W_{RF}$  of the transmitter is defined as

$$W_{RF} = \frac{k S_R E_b}{L_B}, \quad (13)$$

where  $L_B$  is the propagation loss between the transmitter and receiver. It is the ratio of the received signal power to the transmitted signal power.

While UWB enables the use of wideband, its restriction on power density is -41.3 dBm/MHz, which is less than one ten thousandth that of Wi-Fi. Thus, spread spectrum is necessary to ensure SNR. The bandwidth diffused by pseudorandom noise (PN) code is equal to the chip rate  $C_R$ , which is the clock frequency of the PN code.  $W_{DSP}$  is proportionate to the clock frequency of a circuit [13].

The clock frequency of a circuit should be low to reduce  $W_{DSP}$ . However, in order to realize a desired chip rate, a proportionate clock frequency is necessary.  $W_{DSP}$ , which is proportional to  $C_R$ , is expressed as follows.

$$W_{DSP} = \alpha C_R, \quad (14)$$

where  $\alpha$  denotes a constant of proportionality determined by the characteristics of the circuit.

### B. Prototype Communication System

A prototype communication system is created by using GNU Radio [14], which is the development environment of software-defined radio (SDR). The flow diagram of a prototype system in GNU Radio is shown in Fig. 2. Moreover, the specifications of this system are given in Table 1. A 50-cm square 2DC tile is assumed as the communication environment. Owing to the multi-reflection at the edge of the waveguide sheet, a standing wave is generated. Thus, the attenuation from the transmitter to receiver is dependent on the position. In this study, we adopted -30 dB as its representative value.

TABLE I . SPECIFICATIONS OF PROTOTYPE SYSTEM

The parameters of communication environment	
$\sigma_\tau$	10 ns
$L_B$	$1 \cdot 10^{-3}$
$N_0$	-174 dBm/Hz
The parameters of communication system	
$k$	1
$C_R$	50 MHz
$\alpha$	$3.6 \cdot 10^{-10} \text{ J/Hz}$

A digital signal processing method of prototype system resembles that of the TransferJet system. These systems realize high-speed communication at a high symbol rate with single carrier without requiring the high calculation cost of secondary modulation loading. Thus, the value of  $\alpha$  is determined from the data sheet of TransferJet [7]. Notably, the prototype does not equalize the received signal to measure  $\rho_{ISI}$  without a digital correction.

### C. Calculated Result and Evaluation

This subsection aims to calculate EBR at each value of  $E_b/N_0$  and  $\sigma_\tau/S_{DT}$  based on the prototype communication system mentioned in the above subsection and the equations mentioned in Section III-A. A trade-off will be described with the calculation results.

The calculated values of  $R_{EBR}$  at each value of  $E_b/N_0$  and  $\sigma_\tau/S_{DT}$  are shown in Fig. 3. It shows two trade-off factors: one between  $\rho_{ISI}$  and the transmission rate determined by  $S_R (= 1/S_{DT})$  and the other between  $\rho_{SN}$  and  $W_{RF}$ .

In Fig. 3, the relationship between  $\sigma_\tau/S_{DT}$  and  $R_{EBR}$  at  $E_b/N_0 = 14$  demonstrates the first trade-off. The transmission rate increases by increasing  $S_R$ . Thus,  $R_{EBR}$  decreases until  $\sigma_\tau/S_{DT} = 0.35$ . However,  $R_{EBR}$  starts to increase at  $\sigma_\tau/S_{DT} = 0.35$  because  $\rho_{ISI}$  and  $W_{RF}$  increase in  $S_R$ .

The relationship between  $E_b/N_0$  and  $R_{EBR}$  at  $\sigma_\tau/S_{DT} = 0.35$  demonstrates the second trade-off. The transmission rate increases by increasing  $E_b$ . Further,  $\rho_{SN}$  becomes lower than  $10^{-8}$  at  $E_b/N_0 = 14$ .  $R_{EBR}$  starts to increase at  $E_b/N_0 = 14$  because  $W_{RF}$  increases in  $E_b$ .

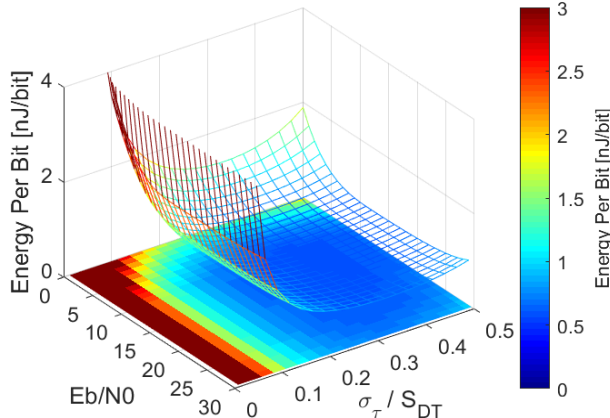


Fig. 3. Calculated values of  $R_{EBR}$  at each value of  $E_b/N_0$  and  $\sigma_\tau/S_{DT}$ . This figure is cited from [7].

The power consumption is 24 mW and the transmission rate is 36 Mbps. These values are calculated using  $E_b$  and  $S_R$  when  $R_{EBR}$  is minimized in Fig. 3. EBR is 0.66 nJ/bit. Moreover, the transmission rate in this study does not consider the influence of the layer above the PHY. Thus, the actual transmission rate will be lower than the calculated results. However, even if the actual transmission rate is assumed to be half of the calculated value, the EBR is lower than the result reported in [3]. This indicates the usefulness of the proposed optimum PHY parameter detection method.

## IV. EXPERIMENT

This section presents the validity of the theoretical equations shown in section III. In particular, we experimentally confirm the relationship between  $\sigma_\tau/S_{DT}$  and  $\rho_{ISI}$ . The transmission rate is calculated based on  $\rho_{ISI}$ . The experimental result presents the feasibility of energy-efficient data transmission in 2DC environments.

### A. Experimental Setup

We measured  $\rho_{ISI}$  for each value of  $S_R$  in two different experimental setups of  $\sigma_\tau$  ( $= 20, 40$  ns) as shown in Fig. 4. Notably, the experimental setup is distinct from the actual usage case since proximity coupling is not used.

A prototype communication system with the function shown in Fig. 2 is implemented by using SDR terminal (Ettus Research, USRP N210) and GNU Radio. However, in the m-PSK modulation/demodulation shown in Fig. 2, 8-PSK is used in this experiment whereas BPSK is assumed in the Section III. The acceptable error vector magnitude of BPSK is the largest in m-PSK. Further,  $\rho_{ISI}$  of BPSK does not change significantly in the range of measurable  $S_R$  whereas 8-PSK changes drastically. Thus, 8-PSK is suitable to confirm the validity of the theoretical equations.

In the setup where  $\rho_{ISI}$  is 20 ns, one of the ports of the divider is connected to the Tx-Port1. The other one is terminated whereas it is connected to the Tx-Port2 through a 16 m coaxial cable when  $\rho_{ISI}$  is 40 ns.

In the experiment, an 8 MB data file was transferred from Tx-Port to Rx-Port of USRP. The BER was calculated based on the transmitted/received data. The BER is determined from the average of BER obtained at each window of window function processing.

Accordingly, 6,400 BER values were obtained from 8 MB (64 Mbit) transmitted/received data files by using the window function (window and step length were 10,000 bits). The average of 6,400 BERs is defined as  $\rho_{ISI}$  at each  $S_R$ . Note that this experiment aims to measure  $\rho_{ISI}$ . The transmitted signal power density was sufficiently large to reduce  $\rho_{SN}$ .

### B. Experimental Results

The experimental results are shown in Fig. 6. The increase in transmission rate slows down after  $S_R$  of 7 MHz when the RMS delay spread is 20 ns. The transmission rate starts to decrease at  $S_R$  of 6 MHz when the RMS delay spread is 40 ns. These experimental results and calculated results are generally

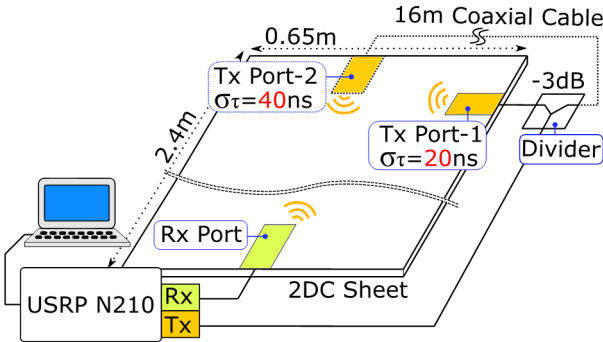


Fig. 5. Experimental setup. This figure is cited from [7].

consistent with each other. This indicates that high-speed communication with high  $S_R$  is feasible in a 2DC tile environment that has an RMS delay spread of 8–10 ns.

Assuming that  $E_b/N_0$  is 15 dB,  $\sigma_\tau$  is 40 ns,  $k$  is 3, and the other parameters follow Table 1, the power consumption  $W$  when  $S_R$  is 6 MHz can be calculated as 21 mW from (12), (13), and (14). EBR is 1.17 nJ/bit. It is higher than the simulated result (0.66 nJ/bit) obtained in Section III-C and lower than the result (1.7 nJ/bit) obtained in the previous work.

These results show that the EBR increases if the delay spread of the waveguide medium increases. Moreover, by adopting the proposed PHY design method, the EBR value becomes lower than the result reported in [3] even if the delay spread increases by 4 times from 10 ns to 40 ns.

## V. CONCLUSION

In this paper, we proposed a method to determine an optimum PHY parameter that minimizes the EBR in 2DC environments. Further, the feasibility of such a method was demonstrated by using experimental and calculated results. Both results

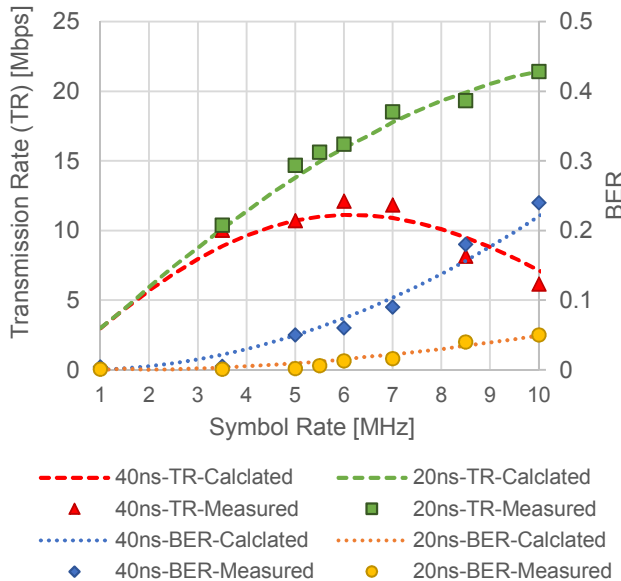


Fig. 6. Experimental result. This figure is cited from [7]

are generally consistent with each other. The EBR decreases to 0.66 nJ/bit when the transmission rate is 36 Mbps with the power consumption of 24 mW. Even if the actual transmission rate at an upper layer of PHY is assumed to be half of the numerical simulation result (36 Mbps), EBR is lower than the result reported in [3].

## ACKNOWLEDGMENT

This work was supported in part by the MIC/SCOPE #155103003 and the JST ACCEL Embodied Media Project (Grant Number JPMJAC1404).

## REFERENCES

- [1] H. Shinoda, Y. Makino, N. Yamahira, and H. Itai, “Surface sensor network using inductive signal transmission layer,” in *Proc. Fourth International Conference on Networked Sensing Systems*, June 2007, pp. 201-206.
- [2] Federal Communications Commission (FCC), “First Report and Order in The Matter of Revision of Part 15 of the Commission’s Rules Regarding Ultrawideband Transmission Systems,” Tech. Rep. ET-Docket 98-153, FCC 02-48, April 2002.
- [3] Y. Masuda, A. Noda, and H. Shinoda, “A low power and high speed data transmission system based on 2D communication,” *IEICE Communications Express*, vol. 5, no. 9, pp. 322-328, Sep. 2016.
- [4] D. Miyashita, K. Agawa, H. Kajihara, K. Sami, M. Iwanaga, Y. Ogasawara, T. Ito, D. Kurose, N. Koide, T. Hashimoto, H. Sakurai, T. Yamaji, T. Kurihara, K. Sato, I. Seto, H. Yoshida, R. Fujimoto, and Y. Unekawa, “A ~70dBm-sensitivity 522Mbps 0.19nJ/bit-TX 0.43nJ/bit-RX transceiver for Transferlet™ SoC in 65nm CMOS,” in *Proc. Symposium on VLSI Circuits Digest of Technical Papers*, Honolulu, June 2012, pp. 74-75.
- [5] J. Lee, Y. Su, and C. Shen, “A Comparative Study of Wireless Protocols: Bluetooth, UWB, ZigBee, and Wi-Fi,” in *Proc. IEEE IECON 2007*, Taipei, Nov. 2007, pp. 46-51.
- [6] A. Okada, A. Noda, and H. Shinoda, “Time domain characteristics of multiple UWB 2D communication tiles,” in *Proc. IEEE/SICE SII 2015*, Nagoya, Dec. 2015, pp. 817-822.
- [7] [in Japanese] Y. Masuda, A. Noda, H. Shinoda, “A Physical Layer Design of High-Speed and Low Power Data Transmission in 2D Communication Environment,” in *Proc. IEICE SRW2016-25*, Tokyo, Mar. 2016, pp. 1-6.
- [8] A. Noda and H. Shinoda, “Active tile for room-size UWB 2-D communication,” in *Proc. IEEE/SICE SII 2015*, Nagoya, Dec. 2015, pp. 668-671.
- [9] C. E. Shannon, “A Mathematical Theory of Communication,” *ACM SIGMOBILE Mobile Computing and Communications Review*, vol.5, no.1, pp. 3-55, Jan. 2001.
- [10] Y. Karasawa, “The Equivalent Transmission-Path Model-A Tool for Analyzing Error Floor Characteristics Due to Intersymbol Interference in Nakagami-Rice Fading Environments,” *IEEE Transactions on Vehicular Technology*, vol.46, no. 1, pp. 194-202, Feb. 1997.
- [11] Y. Karasawa and H. Iwai, “Enhancement of the ETP Model : How to Calculate BER Due to ISI for Wide-Band Digital Transmission in Nakagami – Rice Fading Environments,” *IEEE Transactions on Vehicular Technology*, vol. 49, no. 6, pp. 2113-2120, Nov. 2000.
- [12] Y. Karasawa, *Radiowave propagation fundamentals for digital mobile communications(Second edition)*, pp. 269-285, Tokyo, CORONA PUBLISHING, 2016.
- [13] H. Bogucka and A. Conti, “Degrees of freedom for energy savings in practical adaptive wireless systems,” *IEEE Communications Magazine*, vol. 49, no. 6, pp. 38-45, June 2011.
- [14] GNU Radio , “THE FREE & OPEN SOFTWARE RADIO ECOSYSTEMS” . <http://gnuradio.org/>